# Volume stabilization in human erythrocytes: combined effects of $Ca^{2+}$-dependent potassium channels and adenylate metabolism

Michael V. Martinov*, Victor M. Vitvitsky, Fazoil I. Ataullakhanov

*National Research Center for Hematology, 125167 Moscow, Russia*

## Abstract

A mathematical model describing the possible role of $Ca^{2+}$-dependent $K^+$ channels and adenylate metabolism in volume stabilization of human erythrocytes was developed. The model predicts that the red blood cell volume can be stabilized either dynamically or stationary over a broad range of cell membrane permeabilities to cations. The dynamic stabilization results from the operation of $Ca^{2+}$-dependent potassium channels. The erythrocyte volume changes less than 10% if the membrane permeability changes abruptly to a value in the range from half to sevenfold higher than the normal one. The stationary stabilization is achieved via controlling the adenylate metabolism. The stationary value of cell volume changes less than 10% when the membrane permeability varies from half the normal value to 15-fold higher than the normal value. © 1999 Elsevier Science B.V. All rights reserved.

*Keywords:* Volume regulation; Human erythrocytes; Adenylate metabolism; $Ca^{2+}$-dependent $K^+$ channels; $Na^+/K^+$ ATPase

## 1. Introduction

Circulating erythrocytes must pass through capillaries with diameters smaller than the diameters of these cells. This is achieved due to the erythrocyte's ability to bear substantial deformations. Erythrocyte deformability depends on cell surface-to-volume ratio. Erythrocytes must maintain this ratio at a high level in order to have high deformability [1–3]. The surface-to-volume ratio is known to be remarkably stabilized in human erythrocyte populations [4–7]. The erythrocyte membrane is inextensible; therefore, this ratio is maintained by stabilizing the cell volume. An increase in the cell volume causes a decrease in

___

* Corresponding author. Tel.: + 7-95-212-55-31; fax: + 7-95-212-88-70.

*E-mail address:* mick@blood.ru (M.V. Martinov)

the erythrocyte deformability, and, therefore, deprives its ability to pass through capillaries [2,3]. Moreover, the erythrocyte volume could not be increased > 50−60% without causing the cells to lyse. A decrease in volume also impairs the deformability and rheology of red blood cells by increasing their intracellular viscosity [2,3].

The erythrocyte volume is determined by the non-equilibrium distribution of ions between the cell interior and external medium. This distribution is provided by ion pumps [8−10] and depends on the status of membrane and metabolic systems of the cell. The dynamic equilibrium between ion influxes and effluxes can be readily perturbed by changes in such cellular parameters as enzymatic activities (e.g. $Na^+$, $K^+$-ATPase), medium osmolarity, membrane permeability, etc. It seems plausible that a special mechanism exists for stabilizing red blood cell volume against variations in intracellular parameters, as well as extracellular conditions.

The mechanisms that stabilize the cell volume when medium osmolarity varies are currently being studied extensively [11−14]. Such mechanisms, however, have not yet been found in human erythrocytes. The ion transport systems, such as $K^+−Cl^−$ and $Na^+$, $K^+−2Cl^−$ co-transport, are actively involved in the volume stabilization in a variety of cells, but mature human erythrocytes lack these mechanisms [11,12,15,16]. This may indicate that as plasma osmolarity does not appreciably vary in the circulation, the mechanisms that allow erythrocytes to cope with changes in plasma osmolarity are not necessary. Great variations in the medium composition and pH may also influence volume and volume stabilization [15,17,18], but are also unlikely to occur in vivo. It is natural to expect that non-selective membrane permeability may change during the erythrocyte life span. Severe oxidative stress was shown to change non-selective permeability of red blood cell membranes to cations; this perturbs ion fluxes and, eventually, leads to an increase in cell volume [15,19−21]. Considerable (severalfold) increases in erythrocyte membrane permeability and ion balance impairments were found in some pathologies [15,22−25].

Earlier, we studied volume stabilization in human erythrocytes experiencing changes in non-selective permeability of their cell membranes by analysis of mathematical models constructed to separately estimate the volume-stabilization effects of activation of $Na^+$, $K^+$-ATPase by intracellular $Na^+$[9], operation of $Ca^{2+}$-dependent $K^+$ channels [26,27], and adenylate metabolism [28,29].

In this way, we showed that activation of $Na^+$, $K^+$-ATPase by intracellular $Na^+$ stabilizes the cell volume if changes in cell membrane permeability are relatively small. However, if cell membrane permeability changes three- to fourfold, the erythrocyte volume reaches its critical hemolytic value [9].

$Ca^{2+}$-dependent $K^+$ channels ($K^+$ channels) seem to be the only passive mechanism in mature human erythrocytes that exhibits a high volume-stabilization capacity [30]. In in vitro studies, operation of $K^+$ channels in erythrocytes was shown to decrease their complement-mediated lysis [31,32]. Our theoretical analysis showed that introduction of $K^+$ channels into the model describing osmotic regulation of cell volume, glycolysis, and $Na^+$, $K^+$-ATPase extends severalfold the range of non-selective changes in cell membrane permeability within which the erythrocyte retains its capacity for volume stabilization [26,27]. This stabilization is a fast process, with the characteristic time of the order of several seconds, but it is accompanied by severe changes in intracellular ion (including $Ca^{2+}$) concentrations that may adversely affect the cell.

In erythrocytes, adenylate metabolism is the only metabolic system other than glycolysis that has a potential to directly modify the energy-dependent processes, including active ion transport. It is evident, because adenylate metabolism determines the adenylate pool value and absolute intracellular ATP concentrations. The role of adenylate metabolism in erythrocyte function is not as yet clear. However, a significant increase in the adenylate pool and ATP in erythrocytes observed in a number of pathologies, including leukemia [33,34], sepsis [24], tuberculosis [35], meningococcal infection [36,37], renal insuffi-

ciency [22,38,39], as well as during the red blood cell aging [40], suggests that adenylate metabolism plays a role in cell adaptation to stresses. Using simple qualitative models, we examined the conditions for adenylate metabolism involvement in cell volume stabilization upon changes in the membrane permeability [28,29]. The ideal stabilization of the intracellular ion concentrations and cell volume could be achieved in the models if the rate of transport ATPase was assumed to be proportional to ATP concentration, whereas the rate of AMP decay was assumed to be proportional to ATP and inversely proportional to AMP concentrations. The efficient stabilization of the intracellular ion concentrations and cell volume in our models was achieved owing to an increase in the adenylate pool and ATP concentration (and hence, activation of $Na^+$, $K^+$-ATPase) following the increase in membrane permeability. Consistent with this theoretical result, our experimental studies demonstrated that even a moderate increase in adenylate pool and ATP concentration in human erythrocytes significantly decreased $K^+$ efflux provoked by amphotericin B [41,42]. Adenylate metabolism can provide only slow cell volume stabilization with a characteristic time of approximately 100 h. In previous models, this led to temporal but signifi-

cant deviations of the intracellular ion concentrations and cell volume from their steady-state values after rapid changes in the membrane permeability.

This study is an attempt to extend our previous models to consider both mechanisms for erythrocyte volume stabilization: the passive mechanism involving $Ca^{2+}$-dependent $K^+$ channels and the active mechanism involving adenylate metabolism (Fig. 1). Note that both mechanisms are speculative to a great extent; their experimental substantiation is as yet insufficient. Therefore, this study is the theoretical analysis of the hypothesis of the putative role of $Ca^{2+}$-dependent $K^+$ channels and adenylate metabolism in physiology of human erythrocytes and other cells. The purpose of this study was to understand whether the model extended to describe both stabilization mechanisms mentioned above avoids the drawbacks inherent in the previous models each of which described only one of the two mechanisms.

## 2. Mathematical model

The mathematical model describes ion exchange, osmotic volume regulation, energy and adenylate metabolism in human erythrocyte. The
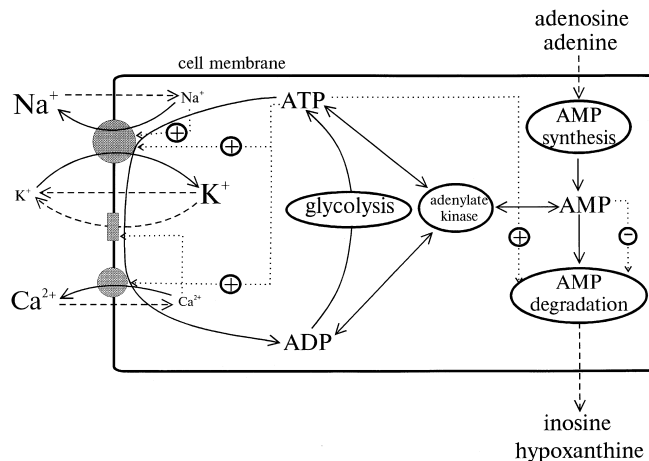


Fig. 1. Schematic representation of the effects of adenylate metabolism and $Ca^{2+}$-dependent potassium channels on transmembrane ion fluxes in human erythrocytes. Solid-colored circles stand for $Na^+/K^+$ and $Ca^{2+}$ ATPases. The rectangle denotes a $Ca^{2+}$-dependent potassium channel. Solid lines show active ion fluxes across the cell membrane and fluxes of metabolites within the cell. Dashed lines indicate passive ion and metabolite fluxes across the cell membrane. Dotted lines indicate regulatory interactions. $+$ and $-$ denote activation and inhibition, respectively.

mathematical model and methods of its investigation are described in Appendix A.

## 3. Results

### 3.1. Dynamic behavior of the model

Numerical analysis of the model revealed the existence of a single stable stationary state in a wide range of parameter changes. Table 1 shows the stationary values of the model variables calculated for the normal physiological values of the model parameters. Intracellular free calcium has a characteristic time of approximately several seconds, glycolytic intermediates change with characteristic times of 0.1 s to 5 min, the characteristic time for energy charge is 1 h; for intracellular sodium and potassium ions, this time is on the order of 10 h, and the pool of adenylates, cell volume, and 2,3-DPG change with the characteristic times in the range 100–300 h.

### 3.2. Role of $Ca^{2+}$-dependent potassium channels in erythrocyte volume stabilization

The contribution of $K^+$ channels into erythrocyte volume stabilization can be evaluated by setting $\alpha_{AMPP} = \alpha_{AMPD} = \nu_S = 0$, because this excludes adenylate metabolism from the model.

Operation of $K^+$ channels leads to volume stabilization when the cell membrane permeability to cations changes in a wide range of its values. This regulatory effect, which is achieved through changes in the intracellular $Ca^{2+}$ concentration in response to non-selective changes in
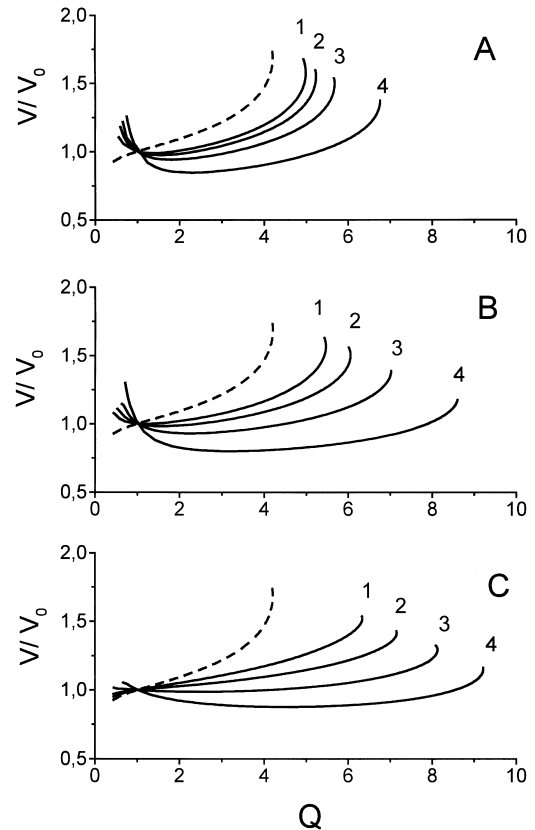


Fig. 2. Dependence of the stationary erythrocyte volume on the normalized value of cell membrane permeability to cations ($Q$) for various values of the $Ca^{2+}$-dependent potassium channel parameters and a constant value of the adenylate pool (the physiological value of the adenylate pool in erythrocytes is 1.75 mM; the equation describing adenylate metabolism is excluded from the model): (a) $N = 1$, $K_{CH} = 39, 29, 19$, and 9 $\mu$M for curves 1, 2, 3, and 4, respectively; (b) $N = 2$, $K_{CH} = 1.9$, 1.5, 1.1, and 0.7 $\mu$M for curves 1, 2, 3, and 4, respectively; and (c): $N = 4$, $K_{CH} = 0.35, 0.33, 0.25$; and 0.22 $\mu$M for curves 1, 2, 3, and 4, respectively. Note that when the constant $K_{CH}$ was varied, the physiological value of passive cell membrane permeability to $K$ ($P_{K0}$) was changed such that the total physiological permeability to $K$ ($P_{K0} + P_{CH}$) remained constant. The dashed line shows the results of solving the model from which equations describing adenylate metabolism and $Ca^{2+}$-dependent potassium channels were excluded.

Table 1
Calculated model variables for normal physiological values of the model parameters

| Variable | Value | Units |
|---|---|---|
| $[Na^+]_i$ | 10 | mM |
| $[K^+]_i$ | 130 | mM |
| $[Ca^{2+}]_i$ | $3 \times 10^{-5}$ | mM |
| $[Ap^-]_t$ | 110 | mM |
| [G6P] | $7 \times 10^{-2}$ | mM |
| [1,3DPG] | $7 \times 10^{-4}$ | mM |
| [2,3DPG] | 5.4 | mM |
| [3PG] | $4.3 \times 10^{-2}$ | mM |
| [ATP] | 1.48 | mM |
| [ADP] | 0.23 | mM |
| [AMP] | $3.7 \times 10^{-2}$ | mM |
| V | 76 | $\mu^3$ |
| $\Delta\varphi$ | $-8.4$ | mV |

the membrane permeability, depends on the parameters of potassium channels (Fig. 2). An increase in their affinity for $Ca^{2+}$ potentiates the effect and can even cause volume over-regulation (Fig. 2, curves 1–4).

The increase in parameter $N$, which characterizes the cooperativity of potassium channels, results in their sharper response to the increased passive permeability of the membrane. For $N = 4$, the contribution of $K^+$ channels in the volume stabilization is evident when the membrane permeability increases, but when it decreases, $K^+$ channels seem to be almost closed (Fig. 2c). All further calculations were performed for $N = 4$ and $K_{CH} = 0.25$ μM (Fig. 2c, curve 3). The results of $K^+$ channels exclusion from the model (by omitting Eq. (3) for calcium exchange and setting $P_{max} = 0$ and $\alpha_{Ca-ATPase} = 0$) are shown by a dashed line in Fig. 2.

Fig. 3 shows how intracellular ion and ATP concentrations in erythrocytes, which either contain or do not contain the $K^+$ channels, change in

response to the changes in the membrane permeability. The cell volume remains almost constant in erythrocytes containing $K^+$ channels, whereas their intracellular $Na^+$ and $K^+$ concentrations change appreciably. These changes are even greater in erythrocytes without $K^+$ channels. An increase in intracellular concentrations of $Na^+$ and $Ca^{2+}$ activates $Na^+/K^+$ ATPase and $Ca^{2+}$ ATPase. An increase in their rates decreases the energy charge and ATP concentration. The characteristic time of operation of the calcium mechanism of stabilization is several seconds (Fig. 4a), this time is required for the cell to establish a new intracellular $Ca^{2+}$ concentration.

### 3.3. Role of adenylate metabolism in erythrocyte volume stabilization

The contribution of adenylate metabolism for the erythrocyte volume stabilization can be evaluated by setting $P_{CH} = \alpha_{Ca-ATPase} = 0$, and excluding Eq. (3) for calcium exchange from the model.
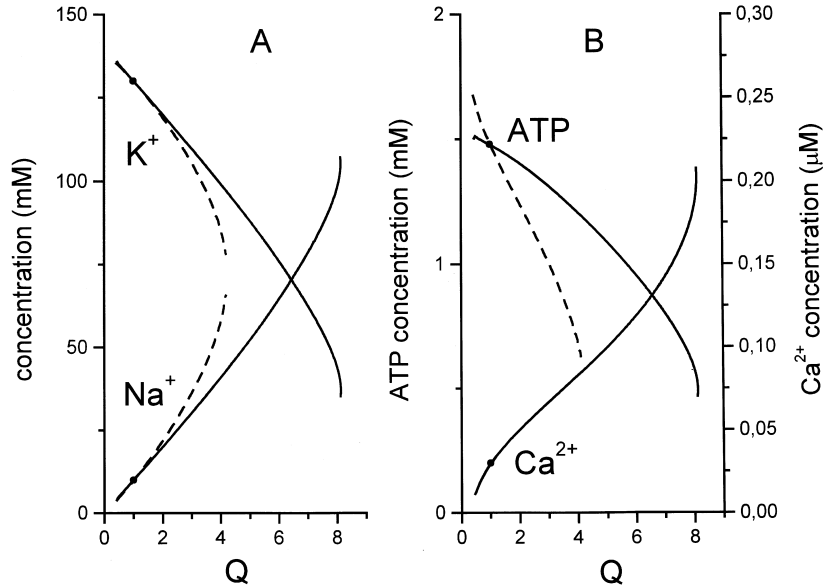


Fig. 3. Dependence of the stationary values of intracellular variables on the normalized cell membrane permeability to cations in the model that did not contain the equations for adenylate metabolism. The parameters of potassium channels used in calculations were $N = 4$ and $K_{CH} = 0.25$ μM; the adenylate pool value was 1.75 mM (a physiological value): (a) $K^+$ and $Na^+$ concentrations; and (b) concentrations of ATP and $Na^{2+}$. The dashed lines show the results of solving the model from which equations describing adenylate metabolism and $Ca^{2+}$-dependent potassium channels were excluded. Circles on curves indicate the physiological stationary state.
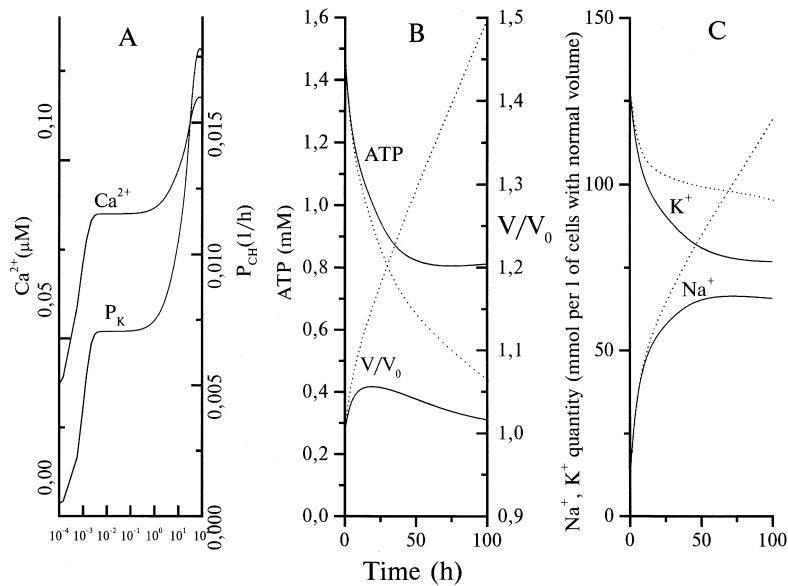
Fig. 4. Dynamics of changes in the values of the model variables after an instantaneous fivefold increase in the cell membrane permeability at $t = 0$ in the model describing the contribution of $Ca^{2+}$-dependent potassium channels: (a) $Ca^{2+}$ concentration and $Ca^{2+}$-dependent potassium channels permeability; (b) ATP concentration and cell volume; and (c) Cell $Na^+$ and $K^+$. The dotted line illustrates the results obtained with the model from which $Ca^{2+}$-dependent potassium channels were excluded

Over a wide range of changes in the membrane permeability, the stationary value of erythrocyte volume can be stabilized efficiently in the absence of potassium channels due to the regulation of adenylate metabolism (Fig. 5a). In this case, volume stabilization results from stabilizing the intracellular $Na^+$ and $K^+$ concentrations (Fig. 6a), which is achieved through regulation of the rate of $Na^+/K^+$-ATPase.

When the adenylate pool is varied it leads to the changes in ATP concentration and in the rate of ATP consumption (Fig. 6b,c). The regulation of the adenylate pool is assumed to be based on the AMP phosphatase inhibition by AMP and its activation by ATP. The AMP deaminase rate sharply increases with increasing AMP. Its dependence on AMP is a sigmoid curve. This determines the greatest possible value of the adenylate pool and the maximum permissible increase in the membrane permeability. Fig. 5a shows the effect of parameter $N_{AMPD}$ on volume stabilization in erythrocytes. For all further calculations we put $N_{AMPD} = 8$, $K^1_{AMPD} = 1$ mM. With these values of the kinetic parameters of AMP deami-

nase, the volume stabilization effect in the model is obvious until the membrane permeability increases 15-fold. If the membrane permeability increases further, $Na^+/K^+$ ATPase requires more ATP to compensate for the increased passive ion fluxes than glycolysis can produce. The volume stabilization effect of adenylate pool regulation is excellent only if the membrane permeability changes slowly, because the rate of adenylate metabolism in erythrocytes is slow. If the membrane permeability changes abruptly, the erythrocyte volume takes transient values that can be far apart from its stationary value, which is stabilized in erythrocyte (Fig. 5b). If an abrupt change in the membrane permeability is significant, the volume can increase by 1.5−2 times and lysis can occur, despite the fact that the stationary value of the volume changes only slightly.

### 3.4. Combined effects of potassium channels and adenylate metabolism

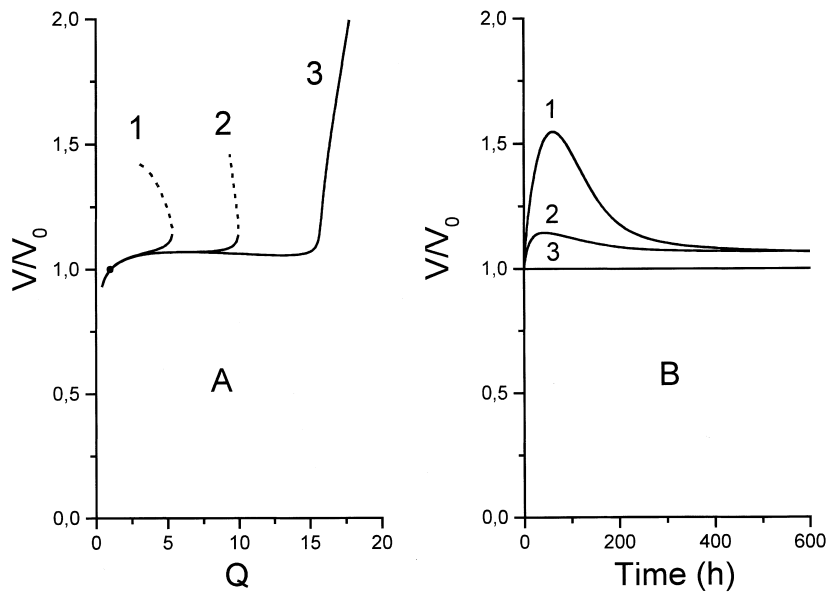The model of volume stabilization describing contributions of both $K^+$ channels and adenylate

Fig. 5. Erythrocyte volume stabilization achievable through regulation of adenylate metabolism ($Ca^{2+}$-dependent potassium channels are excluded from the model). (a) Dependence of the stationary erythrocyte volume on the normalized passive permeability of the cell membrane to cations simulated for various parameters of AMP deaminase: (1) $N = 4$ and $K_{AMPD}^1 = 0.5$ mM; (2) $N = 8$ and $K_{AMPD}^1 = 0.5$ mM; and (3) $N = 8$ and $K_{AMPD}^1 = 1$ mM. The dashed lines show unstable stationary states. Circles on curves indicate the physiological stationary state. (b) Kinetics of erythrocyte volume changes after an instantaneous increase in the cell membrane permeability at $t = 0$ by: (1) 10-fold; (2) fourfold; and (3) without permeability increase.

metabolism does not differ from the previous models in the efficiency of stabilization of the stationary volume, but it provides a much less pronounced overshooting in the cell volume re-

sponse to abrupt changes in the membrane permeability (Fig. 7). This model also describes the stabilization of the stationary values of intracellular ion concentrations, which is provided by
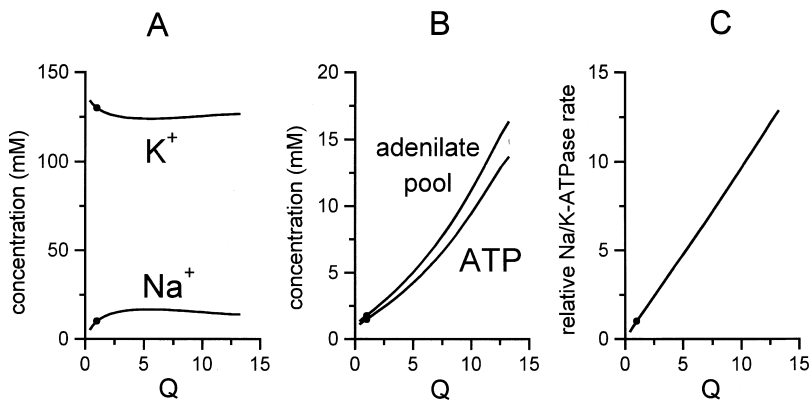


Fig. 6. Dependence of the stationary values of intracellular variables on the normalized value of cell membrane permeability to cations simulated using the model from which equation describing $Ca^{2+}$-dependent potassium channels were excluded and AMP deaminase was assumed to have $N = 8$ and $K_{AMPD}^1 = 1$ mM: (A) $K^+$ and $Na^+$ concentrations; (b) the adenylate pool and ATP concentration; and (c) the relative rate of $Na^+/K^+$ ATPase. Circles on curves indicate the physiological stationary state.
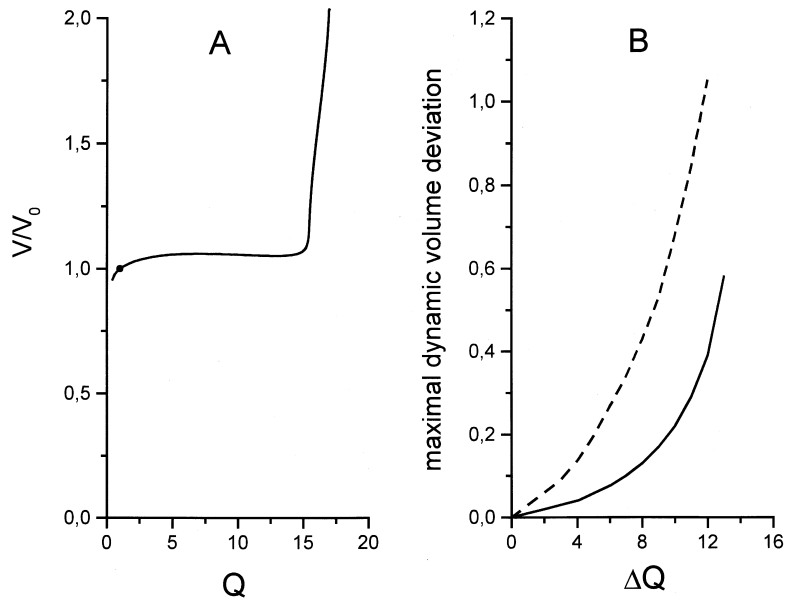
Fig. 7. Erythrocyte volume stabilization in the model describing the contributions of both $Ca^{2+}$-dependent potassium channels and adenylate metabolism control. (a) Dependence of the stationary erythrocyte volume on the normalized passive permeability of the cell membrane to cations. The circle on the curve indicates the physiological stationary state. (b) Effect of an abrupt change in the membrane permeability ($\Delta Q$) on the maximum increase in the erythrocyte volume during transient processes (a solid line). The dashed line illustrates the results obtained with the model from which $Ca^{2+}$-dependent potassium channels were excluded.
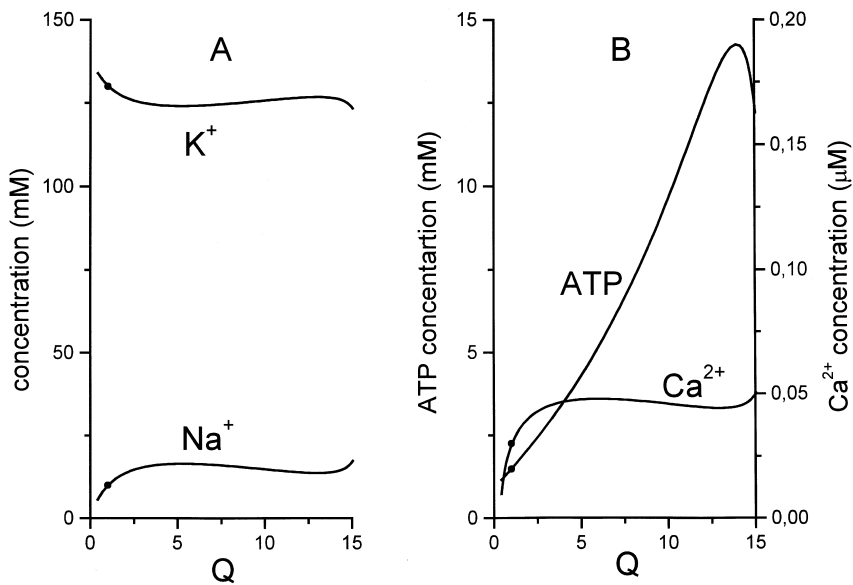


Fig. 8. Dependence of the stationary values of intracellular variables on the normalized value of cell membrane permeability to cations simulated using the model describing the contributions of both $Ca^{2+}$-dependent potassium channels and adenylate metabolism control: (a) $K^+$ and $Na^+$ concentrations and (b) concentrations of ATP and $Ca^{2+}$. Circles on curves indicate the physiological stationary state.
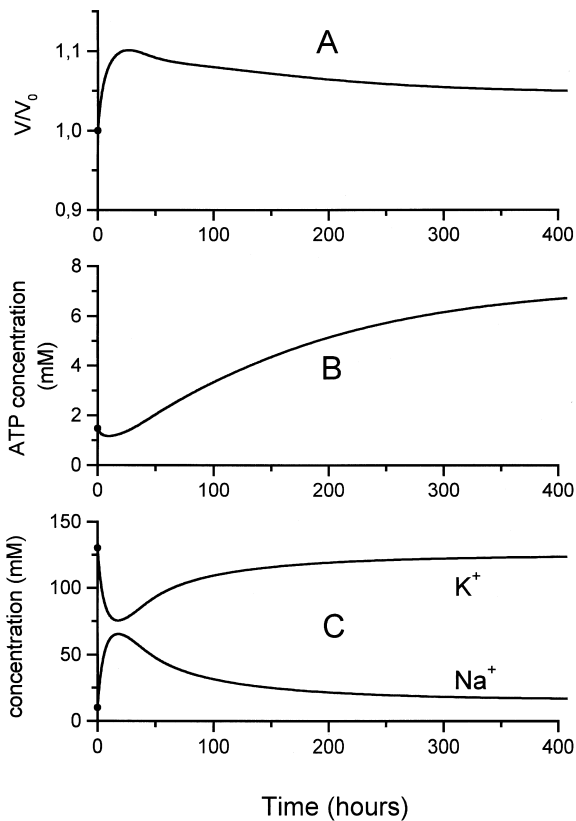
Fig. 9. Dynamics of changes in the values of the model variables after an instantaneous eightfold increase in the cell membrane permeability at $t = 0$ in the model describing the contributions of both $Ca^{2+}$-dependent potassium channels and adenylate metabolism control: (a) cell volume, (b) ATP concentration, (c) $K^+$ and $Na^+$ concentrations. Circles on curves indicate the physiological stationary state.

## 4. Discussion

According to the current view on volume regulation, human erythrocyte maintains its volume at the expense of non-equilibrium partitioning of ions created by transport $Na^+/K^+$-ATPase between the intracellular compartment and the extracellular medium. Oxidative and other stresses increase the non-selective membrane permeability, intracellular $Na^+$, and cell volume. Increased concentrations of intracellular $Na^+$ activate
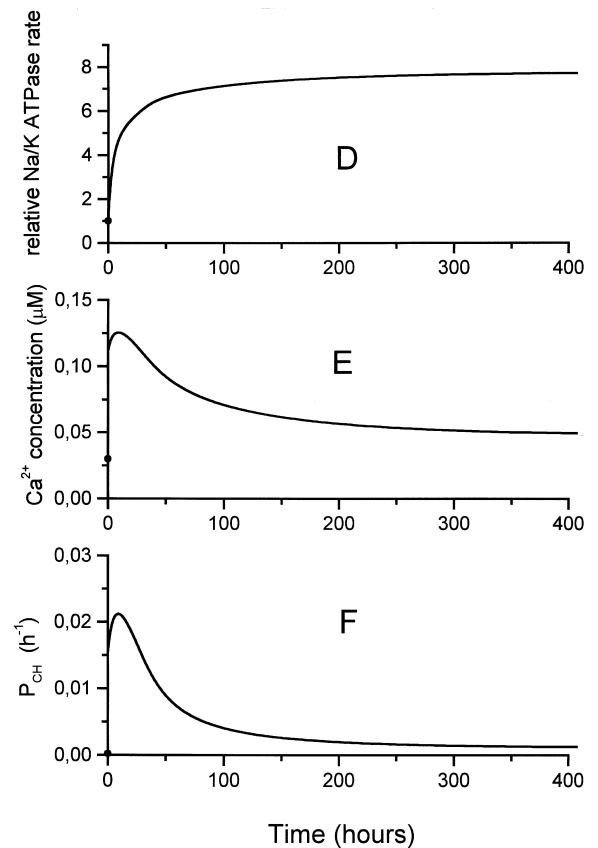


Fig. 10. Dynamics of changes in the values of the model variables after an instantaneous eightfold increase in cell membrane permeability at $t = 0$ in the model describing the contributions of both $Ca^{2+}$-dependent potassium channels and adenylate metabolism control: (d) $Na^+/K^+$ ATPase rate, (e) $Ca^{2+}$ concentration (f) permeability of potassium channels. Circles on curves indicate the physiological stationary state.

the effect of stimulation of transport ATPases by increased ATP concentrations (Fig. 8). Figs. 9 and 10 show the kinetics of various cellular parameters after an abrupt change in the membrane permeability. The important assumption of our model is that the rate of $Ca^{2+}$ ATPase linearly depends on ATP. We also considered a variant of the model in which $Ca^{2+}$ ATPase does not depend on ATP. In this case, the stationary value of the erythrocyte volume is stabilized well, and its changes in response to an abrupt change in the membrane permeability display less pronounced overshooting. However, no satisfactory stabilization of the stationary ion concentrations is achieved.

$Na^+/K^+$-ATPase. This allows the erythrocyte to withstand a decrease in ionic transmembrane gradients and attenuate an increase in cell volume upon membrane impairments. However, this regulation of $Na^+/K^+$-ATPase cannot provide satisfactory volume stabilization in erythrocytes. Model studies showed that a twofold to fivefold non-selective increase in the membrane permeability results in a rapid increase in cell volume and lysis (Fig. 2, dashed lines) [9]. The model that considers adenylate metabolism introduces additional regulation of $Na^+/K^+$-ATPase through changes in ATP concentrations (for which changes in the adenylate pool are responsible). The adenylate pool value depends on the ATP to AMP ratio, which, in turn, depends on the rate of ATP consumption by $Na^+/K^+$-ATPase. This regulation provides good stabilization of intracellular ion concentrations and thereby the erythrocyte volume. The main regulatory effect in the model is exerted by AMP phosphatase. As the rate of AMP deaminase reaction is a sigmoid function of AMP, the role of this enzyme in regulating the adenylate pool is only to determine its maximum value and, hence, the permissible range of membrane permeabilities.

The model predicts the significant growth of ATP concentration with increasing membrane permeability. Such increase in ATP concentration is necessary for volume stabilization only if the rate of transport ATPases is linearly proportional to ATP. If this rate depends on ATP concentration more strongly, then the increase in ATP concentration, which is required to bring about the desirable increase in the rate of ATPases, is less pronounced.

The erythrocyte metabolism is stable only if the rate of adenylate metabolism is low (the characteristic time of approx. 100 h). Hence, adenylate metabolism cannot stabilize the volume rapidly when an abrupt increase in the membrane permeability occurs (Figs. 5b, and 7b). Actually, only stationary values of intracellular ion concentrations and the cell volume are stabilized. During transient processes after an abrupt change in the cell membrane permeability, the volume is stabilized due to operation of $K^+$ channels. Increased concentration of intracellular $Ca^{2+}$ is the signal that the membrane permeability has

changed. Normal concentrations of intracellular $Ca^{2+}$ are maintained at a low level by transport $Ca^{2+}$ ATPase. When the membrane permeability changes non-selectively, intracellular $Ca^{2+}$ increases and $K^+$ channels open. This makes the membrane more permeable to $K^+$ than for $Na^+$ and thereby stabilizes the cell volume. Due to high calcium gradient between cells and extracellular medium, the K channel-dependent volume stabilization is very sensitive to changes in the membrane permeability. The response of $K^+$ channels permeability to changes in the membrane permeability has the characteristic time on the order of several seconds, which is determined by the rate of an increase in the intracellular $Ca^{2+}$ concentration. Therefore, $K^+$ channels can stabilize the erythrocyte volume even if the cell membrane permeability changes abruptly. This model differs from the previous models of volume stabilization relying on the operation of $K^+$ channels in that: (1) the rate of $Ca^{2+}$ ATPase is assumed to depend on ATP; and (2) the permeability of potassium channels is assumed to depend on $Ca^{2+}$ concentration cooperatively. It appeared that the $K^+$ channel cooperativity plays an important part in the erythrocyte volume stabilization (Fig. 2), extending the permissible range of changes in the cell membrane permeability by 1.5−2 times. Patch-clamp studies with fragments of erythrocyte membranes showed that the permeability of potassium channels linearly depends on $Ca^{2+}$ concentration in the range from 0.5 to 100 $\mu M$ [43]. In the model, this corresponds to $N = 1$. However, the dependence of potassium channels on $Ca^{2+}$ at concentrations $< 0.5$ $\mu M$ (typical intracellular concentrations) has not been studied. Moreover, the data of the study cited above suggest that the permeability of potassium channels depend on $Ca^{2+}$ even stronger in the range of low (intracellular) $Ca^{2+}$ concentrations than in the range studied. Therefore, the model assumption that $N = 4$ does not contradict the known experimental data on the kinetics of potassium channels. For the values of $N$ and $K_{CH}$ chosen in the model, the half-maximum activation of potassium channels is achieved at a concentration of intracellular $Ca^{2+}$ of 1.3 $\mu M$, in a good agreement with the data available in the literature [43−45]. A serious drawback to the erythro-

cyte volume stabilization based on the operation of $K^+$ channels is that intracellular concentrations of ions, especially $Ca^{2+}$, can change significantly and produce adverse effects on cells.

Our results demonstrate that combining the two mechanisms of volume stabilization (potassium channels and adenylate metabolism) in one model eliminates the disadvantages of individual mechanisms and provides volume stabilization of the erythrocyte independent of whether its state is stationary or transient. The dynamic stabilization of cell volume during transient processes elicited by an abrupt change in the cell membrane permeability is possible in the model due to the operation of potassium channels, whereas the stabilization of the stationary values of intracellular ion concentrations is maintained due to adenylate metabolism control. The model assumption that the rate of transport $Ca^{2+}$-ATPase is proportional to ATP concentration is a prerequisite for stabilization of intracellular ion concentrations. Unfortunately, there are no reliable data on the dependence of the rate of this ATPase on the ATP concentration under intracellular conditions. Analysis of the model shows that the volume stabilization can be satisfactory even if the rate of $Ca^{2+}$-ATPase does not depend on ATP concentration. However, the intracellular ion concentrations are not stabilized in this case. Interestingly, the functional roles of $K^+$ channels and adenylate metabolism in erythrocytes are still unclear.

**Acknowledgements**

**Appendix A. Mathematical model**

*A.1. Ion balance and the erythrocyte volume*

Basic equations describing the dynamics of $Na^+$ and $K^+$ concentrations and the erythrocyte volume were introduced in Brumen and Heinrich [46] and Werner and Heinrich [47]. Ion balance and the erythrocyte volume are described by a set of equations based on Brumen and Heinrich [46], Werner and Heinrich [47] and Ataullakhanov et al. [26]:

$$\frac{\mathrm{d}}{\mathrm{d}t}\left([K^+]_i \frac{V}{V_0}\right) = 2\nu_{Na/K\text{-ATPase}}$$

$$+ (P_K + P_{CH})\frac{\frac{\Delta\varphi F}{RT}}{\exp\left(\frac{\Delta\varphi F}{RT}\right) - 1}$$

$$\left([K^+]_e - [K^+]_i \exp\left(\frac{\Delta\varphi F}{RT}\right)\right) \tag{1}$$

$$\frac{\mathrm{d}}{\mathrm{d}t}\left([Na^+]_i \frac{V}{V_0}\right) = -3\nu_{Na/K\text{-ATPase}}$$

$$+ P_{Na}\frac{\frac{\Delta\varphi F}{RT}}{\exp\left(\frac{\Delta\varphi F}{RT}\right) - 1}\left([Na^+]_e\right.$$

$$\left. - [Na^+]_i \exp\left(\frac{\Delta\varphi F}{RT}\right)\right) \tag{2}$$

$$\frac{\mathrm{d}}{\mathrm{d}t}\left([Ca^{2+}]_i \frac{V}{V_0}\right) = -2\nu_{Ca\text{-ATPase}}$$

$$+ P_{Ca}\frac{2\frac{\Delta\varphi F}{RT}}{\exp\left(2\frac{\Delta\varphi F}{RT}\right) - 1}$$

$$\times \left([Ca^+]_e - [Ca^{2+}]_i \exp\left(2\frac{\Delta\varphi F}{RT}\right)\right) \tag{3}$$

$$[K^+]_i + [Na^+]_i + [A_p^-]_i + [A_n^{z-}]_i$$
$$= [K^+]_e + [Na^+]_e + [A_p^-]_e + [A_n^{z-}]_e \tag{4}$$

$$[K^+]_i + [Na^+]_i - [A_p^-]_i - Z\cdot[A_n^{z-}]_i = 0 \tag{5}$$

$$\frac{[A_p^-]_i}{[A_p^-]} = \exp\left(\frac{\Delta\varphi F}{RT}\right) \tag{6}$$

where $V$ and $V_0$ are the current and the normal physiological cell volumes; $\Delta\varphi$ is the transmembrane potential; $F$ is the Faraday constant; $R$ is the universal gas constant; $T$ denotes absolute temperature; $P_K$, $P_{Na}$, $P_{Ca}$ are the passive permeability of the erythrocyte membrane for $K^+$, $Na^+$, $Ca^{2+}$, respectively; $P_{CH}$ is the permeability of $K^+$ channels; $\nu_{Na/K\text{-}ATPase}$ and $\nu_{Ca\text{-}ATPase}$ denote the rates of transport $Na^+/K^+$ and $Ca^{2+}$ ATPases (ion pumps), respectively; $[A_p^-]$ and $[A_n^{Z-}]$ are the concentrations of permeable ($Cl^-$ and $HCO_3^-$) and impermeable anions, respectively; subscripts i and e denote intra- and extracellular variables and parameters, respectively; $Z^-$ is the average negative charge of the impermeable anions.

The following values of the ion concentrations [48–51,23], normal rate of transport $Na^+/K^+$-ATPase [23,50,52,53], and intracellular ATP concentration [22,50,54,55] were estimated from the literature: $[K^+]_e = 5$ mM, $[Na^+]_e = 145$ mM, $[A_p^-]_e = 150$ mM, $[K^+]_i = 130$ mM, $[Na^+]_i = 10$ mM, $[A_p^-]_i = 110$ mM, $\nu_{Na/K\text{-}ATPase} = 0.65$ mM/h, $[ATP] = 1.48$ mM. Normal physiological values of the remaining steady-state parameters are readily determined from Eqs. (1)–(6): $[A_n^{Z-}]_i = 50$ mM, $Z = 0.6$, $P_K = P_{K0} = 1.24 \times 10^{-2}$ 1/h, $P_{Na} = P_{Na0} = 1.22 \times 10^{-2}$ 1/h, $\Delta\varphi = -8.4$ mV. $[Ca^{2+}]_e = 1$ mM and $[Ca^{2+}]_i = 0.03$ μM were taken from Simons [56] and Wiley and Shaller [57]. Transport $Ca^{2+}$-ATPase was assumed to operate at a rate of 5.2 μM/h [58]. Eq. (3) can be used to estimate the normal physiological value of passive permeability of the erythrocyte membrane to $Ca^{2+}$: $P_{Ca} = P_{Ca0} = 0.76 \times 10^{-2}$ 1/h.

Eqs. (1)–(3) describe active and passive $K^+$, $Na^+$ and $Ca^{2+}$ fluxes across the erythrocyte membrane. Passive ion fluxes are described using Goldman's approach. The rates of $Na^+/K^+$ and $Ca^{2+}$ ATPase reactions are written as

$$\nu_{Na/K\text{-}ATPase} = \alpha_{Na/K\text{-}ATPase}[Na^+]_i[ATP] \qquad (7)$$

$$\nu_{Ca\text{-}ATPase} = \alpha_{Ca\text{-}ATPase}\left(\frac{[Ca^{2+}]}{[Ca^{2+}] + K_{Ca\text{-}ATPase}}\right)^2$$
$$\times [ATP] \qquad (8)$$

where $\alpha_{Na/K\text{-}ATPase} = 0.044$ 1/(mM·h), $\alpha_{Ca\text{-}ATPase} = 5$ 1/h are activities of $Na^+/K^+$ and $Ca^{2+}$-ATPases, $K_{Ca\text{-}ATPase} = 1.1$ μM.

The important model assumption is that the rates of ion transport ATPases depend on the ATP concentration. Most of the published studies of the kinetics of transport $Na^+$, $K^+$ and $Ca^{2+}$–ATPases contain the Michaelis constant for ATP, which is lower than the intracellular ATP concentration. These results, however, were obtained using the isolated enzymes and were often performed with the reconstructed systems (such as erythrocyte ghosts). Therefore, a possible regulatory role of some intracellular factors, such as adenylates other than ATP (ADP and AMP), could have been missed. Kennedy et al. [59] showed that the Michaelis constant for the $Na^+$, $K^+$–ATPases in red blood cells depend on the ratio of ATP and ADP concentrations. Our previous work with native human erythrocytes demonstrated that the total rate of ATP consumption grows sharply with the growing ATP concentration [60]. We also showed that even a moderate increase in ATP concentration significantly decreased the $K^+$ efflux provoked by amphotericin B [41,42]. It appears that in native erythrocytes the rate of transport ATPases might be significantly influenced by the ATP concentration.

The following expression

$$P_{CH} = P_{max}\left(\frac{[Ca^{2+}]}{[Ca^{2+}] + K_{CH}}\right)^N \qquad (9)$$

where $P_{max}$ is the maximal permeability of $K^+$ channels, $N$ is the cooperativity parameter, $K_{CH}$ is the affinity constant, shows how the permeability of $K^+$ channels depends on the concentration of $Ca^{2+}$. It was obtained on the basis of the data described in [43–45]. Here, $P_{max} = 1.7$ 1/h. The parameters $N$ and $K_{CH}$ could not be unambiguously determined from these experimental data. We, therefore, varied the values of these parameters when analyzing the model. Eq. (4) describes osmotic balance in the system. The erythrocyte is considered as an ideal osmometer. Eq. (5) describes the electroneutrality of the cell content and takes into account the contributions of sodium

and potassium ions, anions like $HCO_3^-$ and $Cl^-$, which permeate the membrane, and polyvalent anions (e.g. hemoglobin and 2,3-diphopho-glycerate) for which the membrane is imperme-able. The erythrocyte membrane permeability to $HCO_3^-$ and $Cl^-$ is high [61,62]; therefore, Eq. (6) describes the equilibrium for these anions between the intracellular and extracellular com-partments in the presence of the transmembrane potential. The medium osmolarity was assumed to be determined only by the extracellular concen-trations of permeating ions ($[A_n^{Z-}]_e = 0$). As ear-lier, we consider non-selective changes in the erythrocyte membrane permeability to cations (which can be caused by oxidative or other stresses within a body) assuming that $P_K = P_{K0} + \Delta P$; $P_{Na} = P_{Na0} + \Delta P$; $P_{Ca} = P_{Ca0} + \Delta P$, where $\Delta P$ de-notes the value of a change in the membrane permeability and introducing the normalized value of cell membrane permeability to cations $Q$: $Q = P_{Na}/P_{Na0} \approx P_K/P_{K0} \approx (P_{Ca}/P_{Ca0} + 1)/2$, because $P_{Na0} \approx P_{K0} \approx 2P_{Ca0}$.

## A.2. Energy metabolism

### A.2.1. The ATPases

Eqs. (7) and (8) describe the rates of ATP consumption by transport $Na^+/K^+$ and $Ca^{2+}$ ATPases, respectively. The sum of the normal values of their rates in erythrocytes is significantly lower than the rate of ATP production in glycoly-sis. To balance the ATP production, an ATPase other than transport ATPases was included in the model:

$$v_{ATPase} = \alpha_{ATPase}[ATP]/([ATP] + K_{ATPase}) \quad (10)$$

where $\alpha_{ATPase} = 0.88$ mM/h, $K_{ATPase} = 0.1$ mM.

## A.3. Glycolysis

ATP consumed by the transport ATPases and other ATP-consuming systems is replenished in erythrocytes by glycolysis. In this work we con-sider the reactions of glycolysis in the form, which is more complete than that presented in our previous studies [27−29]. Specifically, here we in-troduce additional reactions describing the kinet-

ics of concentrations of 1,3-diphosphoglycerate, 2,3-diphosphoglycerate and 3-phosphoglycerate. This reactions allow more complete description of the transition processes in the model (below). The phosphohexoisomerase, aldolase, triosophosphate isomerase, glyceraldehydephosphate dehydroge-nase, phosphoglycerate mutase and enolase are highly active in erythrocytes, so the equations for these reactions were replaced by equilibrium rela-tionships between the corresponding metabolites. This, however, could not be done for the phos-phoglycerate kinase reaction, which is coupled to the 2,3-diphosphoglycerate bypass. The concen-trations of NAD, NADPH, and phosphate were assumed to be constant. The resulting description of the glycolysis in our model is given by the following set of equations:

$$\frac{d}{dt}\left([G6P]\frac{V}{V_0}\right) = \frac{v_{HK} - v_{PFK}}{D_1} \quad (11)$$

$$\frac{d}{dt}\left([1,3DPG]\frac{V}{V_0}\right) = \frac{2v_{PFK} - v_{DPGM} - v_{PGK}}{D_2} \quad (12)$$

$$\frac{d}{dt}\left([2,3DPG]\frac{V}{V_0}\right) = v_{DPGM} - v_{DPGP} \quad (13)$$

$$\frac{d}{dt}\left([3PG]\frac{V}{V_0}\right) = \frac{v_{PGK} + v_{DPGP} - v_{PK}}{D_3} \quad (14)$$

$$([ATP] + [ADP] + [AMP])\frac{V}{V_0} = a \quad (15)$$

$$\frac{[ADP]^2}{[AMP][ATP]} = 1 \quad (16)$$

Here, the expressions

$$D_1 = 1 + 1/K_{PHI}; D_2$$
$$= 1 + \frac{1}{K_{GAPDH}}\left(1 + \frac{1}{K_{TPI}}\left(1 + \frac{2 \cdot [1,3DPG]}{K_{GAPDH}K_{ALD}}\right)\right);$$
$$D_3 = 1 + \frac{1}{K_{ENO}}\left(1 + \frac{1}{K_{PGM}}\right)$$

result from exclusion of the fast intermediates of glycolysis. $K_{PHI} = 3$, $K_{ALD} = 0.012$ mM, $K_{TPI} = 0.3$, $K_{GAPDH} = 0.75$, $K_{PGM} = 0.14$, $K_{ENO} = 1.7$ were obtained from Erlich et al. [63].

[G6P], [1,3DPG], [2,3DPG], [3PG], [2PG], [PEP] correspond to the intracellular concentrations of glucose-6-phosphate, 1,3-diphosphoglycerate, 2,3-diphosphoglycerate, 3-phosphoglycerate, 2-phosphoglycerate, and phosphoenolpyruvate, respectively. Symbol $a$ corresponds to the total adenylate content of a cell (the adenylate pool). $v_{HK}$, $v_{PFK}$, $v_{PGK}$, $v_{DPGM}$, $v_{DPGP}$, and $v_{PK}$ denotes the reaction rates of hexokinase, phosphofructokinase, phosphoglycerate kinase, diphosphoglycerate mutase, diphosphoglycerate phosphatase, and pyruvate kinase, respectively. Adenylate kinase reaction is believed to be in equilibrium because the activity of adenylate kinase in erythrocytes is high [64]. Eq. (16) describes the adenylate kinase equilibrium, with the equilibrium constant equal to 1.

Eqs. (11)–(16) do not contain such variables as the concentrations of glucose, pyruvate, and lactate. Lactate dehydrogenase reaction was also excluded from our consideration. Normally, in vivo erythrocyte glycolysis is always saturated with glucose. The concentrations of lactate and pyruvate, being controlled at the whole-body level, do not depend on the rate of glycolysis in erythrocytes.

The expressions for rates of enzymatic reactions in this model are taken from Ataullakhanov et al. [29], Erlich et al. [63] and Joshi and Palsson [65]:

$$v_{HK} = \alpha_{HK} \frac{[ATP]/K_{HK}^1}{1 + [ATP]/K_{HK}^1 + [G6P]/K_{HK}^2} \quad (17)$$

$\alpha_{HK} = 12.2 \, \text{mM}/h, K_{HK}^1 = 1.22 \, \text{mM}, K_{HK}^2$

$\qquad = 6 \cdot 10^{-2}$ mM.

$v_{PFK} = \alpha_{PFK}$

$$\frac{[ATP][G6P]/K_{PHI}}{(K_{PFK}^3 + [ATP])(K_{PFK}^2 + [G6P]/K_{PHI})}$$

$$\times \frac{[1/(1 + [AMP]/K_{PFK}^4) + 2[AMP]/(K_{PFK}^4 + [AMP])]}{\left[1 + L \frac{(1 + [ATP]/K_{PFK}^5)^4}{(1 + [AMP]/K_{PFK}^4)^4} \times (1 + [G6P]/K_{PHI} K_{PFK}^6)^4\right]} \quad (18)$$

$\alpha_{PFK} = 380$ mM/h, $L = 10^8$, $K_{PFK}^1 = 10$ mM, $K_{PFK}^2 = 0.1$ mM, $K_{PFK}^3 = 2$ mM, $K_{PFK}^4 = 10^{-2}$ mM, $K_{PFK}^5 = 0.1$ mM, $K_{PFK}^6 = 3.7 \cdot 10^{-4}$ mM, $K_{PHI} = 3$.

$$v_{DPGM} = \alpha_{DPGM} \frac{[1,3DPG]}{K_{DPGM}^1 + K_{DPGM}^2[1,3DPG] + [2,3DPG]} \quad (19)$$

$\alpha_{DPGM} = 3892$ mM/h; $K_{DPGM}^1 = 0.04$ mM; $K_{DPGM}^2 = 0.013$ mM;

$$v_{DPGP} = v_{DPGP} \frac{[2,3DPG]}{[2,3DPG] + K_{DPGP}^1} \times \left(1 + \frac{[2PG] + [3PG]}{K_{DPGP}^2}\right) \quad (20)$$

$\alpha_{DPGP} = 0.52$ mM/h; $K_{DPGP}^1 = 0.02$ mM; $K_{DPGP}^2 = 0.006$ mM;

$v_{PGK} = \alpha_{PGK}$

$$\frac{([1,3DPG][ADP] - [3PG][ATP]/K_{PGK}^3)/K_{PGK}^1 K_{PGK}^2}{1 + [ATP]/K_{PGK}^5 + [ADP]/K_{PGK}^2 + A[1,3DPG]/K_{PGK}^1 + B[3PG]/K_{DPGP}^6} \quad (21)$$

$$A = (K_{PGK}^2 + [ADP] + [ATP]K_{PGK}^4/K_{DPGK}^5) / K_{PGK}^2$$

$$B = (K_{PGK}^7 + [ATP] + [ADP]K_{PGK}^7/K_{PGK}^2) / K_{PGK}^5$$

$\alpha_{PGK} = 7330$ mM/h; $K_{PGK}^1 = 0.0022$ mM; $K_{PGK}^2 = 0.14$ mM; $K_{PGK}^3 = 380$; $K_{PGK}^4 = 0.3$ mM; $K_{PGK}^5 = 0.27$ mM; $K_{PGK}^6 = 1.4$ mM; and $K_{PGK}^7 = 0.4$ mM;

$$\nu_{PK} = \alpha_{PK} \frac{[PEP][ADP]/K_{PK}^1 K_{PK}^2}{1 + [PEP]/K_{PK}^1 + ADP/K_{PK}^2} \quad (22)$$
$$+ ATP/K_{PK}^3 + [PEP][ADP]$$
$$/K_{PK}^1 K_{PK}^2$$

$\alpha_{PK} = 120$ mM/h; $K_{PK}^1 = 0.05$ mM; $K_{PK}^2 = 0.3$ mM; and $K_{PK}^3 = 0.35$ mM;

### A.4. Adenylate metabolism

The adenylate and energy metabolisms are closely linked. Adenylate metabolism in the erythrocyte serves to synthesize AMP from adenine or adenosine and to irreversibly degrade AMP [54,66−69]. In the model, adenylate metabolism is represented only by a reaction of irreversible AMP synthesis and two irreversible reactions of AMP degradation.

The dynamics of adenylate nucleotide concentrations can be found by solving the following set of equations describing interaction of adenylate and energy metabolisms:

$$\frac{d}{dt}\left([ATP]\frac{V}{V_0}\right) = \nu_{PGK} + \nu_{PK} - \nu_{PFK} - \nu_{HK}$$
$$- \nu_{Na/K\text{-}ATPase} - \nu_{Ca\text{-}ATPase}$$
$$- \frac{3}{2}\nu_s - \nu_{AK} \quad (23)$$

$$\frac{d}{dt}\left([ADP]\frac{V}{V_0}\right) = -\nu_{PGK} - \nu_{PK} - \nu_{PFK} - \nu_{HK}$$
$$+ \nu_{Na/K\text{-}ATPase} + \nu_{Ca\text{-}ATPase}$$
$$+ \nu_{ATPase} + \nu_s + 2\nu_{AK} \quad (24)$$

$$\frac{d}{dt}\left([AMP]\frac{V}{V_0}\right) = \frac{3}{2}\nu_s - \nu_{AMPP} - \nu_{AMPD} - \nu_{AK}$$
$$(25)$$

$$\frac{[ADP]^2}{[AMP][ATP]} = 1 \quad (26)$$

$\nu_S$ is the rate of AMP production in adenosine kinase and adenine phosphoribosyl transferase reactions. We assume that the rates of these two

reactions are equal and constant. Eqs. (23)−(25) are written according to the stoichiometry of adenylate formation and disappearance during AMP synthesis from adenine and adenosine. $\nu_{AK}$ is the rate of adenylate kinase reaction; $\nu_{AMPP}$ and $\nu_{AMPP}$ denote the rates of AMP phosphatase and AMP deaminase. $\nu_S$ is assumed to be constant ($\nu_S = $ const $= 0.04$ mM/h). This low rate of adenylate metabolism in human erythrocytes (approx. 4% of glycolytic flux) is optimum for maintaining the stable state of cellular metabolism [28]. Unlike our earlier models [28,29], this model includes two enzymes involved in degradation of the adenylate pool: AMP phosphatase and AMP deaminase. This is consistent with the known data on adenylate metabolism in human erythrocytes. The rate of AMP deaminase reaction is taken as:

$$\nu_{AMPD} = \alpha_{AMPD}\left(\frac{[AMP]}{[AMP] + K_{AMPD}^1}\right)^{N_{AMPD}} \quad (27)$$

where $\alpha_{AMPD} = 100$ mM/h [70,71]. This is the general form of sigmoid dependence of the reaction rate on the concentration of AMP known from the literature where $N_{AMPD}$ is approximately 2 and $K_{AMPD}^1$ is in the range 0.4−2.0 mM [70,72,73]. However, the in vitro kinetics of this enzyme can differ from its kinetics within a cell where such effectors as ATP, 2,3-DPG, orthophosphate are present [70,72,73]. Therefore, the AMP deaminase parameters were varied in the model. As follows from the sigmoid kinetics of AMP deaminase, it does not operate at normal intracellular concentrations of AMP. We suggest that under physiological conditions, AMP degradation is regulated by AMP phosphatase. The rate of AMP phosphatase reaction is taken as:

$$\nu_{AMPP} = \alpha_{AMPP}\left(1 + \frac{[ATP]}{K_{AMPP}^1}\right)$$
$$/\left(1 + \frac{K_{AMPP}^2}{[AMP]} + \frac{[AMP]}{K_{AMPP}^3}\right) \quad (28)$$

$\alpha_{AMPP} = 1$ mM/h, $K_{AMPP}^1 = 1$ mM, $K_{AMPP}^2 = 0.01$ mM, $K_{AMPP}^3 = 0.05$ mM.

This expression makes the rate of AMP phosphatase reaction directly proportional to ATP

concentration and inversely proportional to AMP concentration in a broad range of AMP and ATP concentrations. Such dependence provides the most effective stabilization of the intracellular ion concentrations and the cell volume when membrane permeability is perturbed [28,29]. The value of $\alpha_{AMPP}$ was chosen so that the model provided the normal stationary concentration for adenine nucleotides.

Both enzymes that destroy intracellular AMP, the AMP phosphatase and AMP deaminase, have complex kinetics, which depend on concentrations of several metabolites, as well as their ratios. The exact details of these relations and their physiological roles are not yet known. The in vitro rates for AMP phosphatase and AMP deaminase enzymes isolated from liver have a bell-shaped dependency on the energy charge [74,75]. Since the increase in energy charge means the increase in ATP concentration and decrease in AMP concentration, the rates of AMP phosphatase and AMP deaminase are indeed proportional to the ATP concentration and are inversely proportional to the AMP concentration for some range of adenine nucleotides concentrations. The important role of this dependence for regulation of adenine nucleotides is supported by the observed high rate of the adenosine turnover between the erythrocytes and plasma [76].

The equilibrium in adenylate kinase reaction allows us to exclude the rate of adenylate kinase from Eqs. (23)−(26). The final set of the model equations comprises Eqs. (1)−(6), Eqs. (11)−(14), and Eqs. (23)−(26). For the numerical analysis of the model we used a software package DBSolve [77]. In this program the transient behavior of models is simulated by ordinary differential equations integration using an original algorithm based on the Gear procedure [78]. DBSolve also calculates the steady-state solution along a parameter range using the original parameter continuation algorithm.

## References

[1]  W.H. Reinhardt, C. Huang, M. Vayo, G. Norwich, S. Chien, S. Skalak, Biorheology 28 (1991) 537−549.
[2]  F.I. Ataullakhanov, V.M. Vitvitsky, I.L. Lisovskaya, E.G. Tuzhilova, Biophysics (Moscow) 39 (1994) 672−680.
[3]  I.L. Lisovskaya, F.I. Ataullakhanov, E.G. Tuzhilova, V.M. Vitvitsky, Biophysics (Moscow) 39 (1994) 893−901.
[4]  P.B. . Canham, Circ. Res. 25 (1969) 39−48.
[5]  G.B. Nash, S.J. Wyard, Biorheology 17 (1980) 479−489.
[6]  O. Lindercamp, H. Meiselman, Blood 59 (1982) 1121−1127.
[7]  V.L. Lew, J.E. Raftos, M. Sorette, R.M. Bookchin, N. Mohandas, Blood 86 (1995) 334−341.
[8]  D.C. Tosteson, J.F. Hoffman, J. Gen. Physiol. 44 (1960) 169−194.
[9]  I.A. Moroz, F.I. Ataullakhanov, A.B. Kiyatkin, A.V. Pichugin, V.M. Vitvitsky, Biol. Membr. 6 (1989) 409−419.
[10] V.L. Lew, C.J. Freeman, O.E. Ortiz, R.M. Bookchin, J. Clin. Invest. 87 (1991) 100−112.
[11] E.K. Hoffmann, L.O. Simonsen, Physiol. Rev. 69 (1989) 315−382.
[12] B. Sarkadi, J.C. Parker, Biochim. Biophys. Acta 1071 (1991) 407−427.
[13] S.N Orlov, K.N. Novikov, Fiziol. Zh. SSSR im. I.M. Sechenova (in Russian) 82 (1996) 1−15.
[14] S.N Orlov, S.L. Aksentsev, K.N. Novikov, S.V. Konev, Fiziol. Zh. SSSR im. I.M. Sechenova (in Russian) 83 (1997) 1−18.
[15] J. Stuart, J.C. Ellory, Clin. Hemorheol. 7 (1987) 827−851.
[16] G.W. Stewart, Baillieres Clin. Haematol. 6 (1993) 371−399.
[17] V.L. Lew, R.M. Bookchin, J. Membr. Biol. 92 (1986) 57−74.
[18] A. Joshi, B.O. Palsson, J. Theor. Biol. 142 (1990b) 69−85.
[19] F.I. Ataullakhanov, V.M. Vitvitskii, A.M. Zhabotinskii, A.B. Kiyatkin, A.V. Pichugin, E.I. Sinauridze, Biochemistry (Moscow) 51 (1986) 1562−1770.
[20] B. Deuticke, B. Heller, C.W.M. Haest, Biochim. Biophys. Acta 854 (1986) 169−183.
[21] R.P. Hebbel, N. Mohandas, Biophys. J. 60 (1991) 712−715.
[22] H.J. Kramer, D. Gospodinov, F. Kruck, Nephron 16 (1976) 344−358.
[23] M.A. Mir, H. Bobinski, Clin. Sci. Mol. Med. 48 (1975) 213−218.
[24] H. Illner, G.T. Shires, Circ. Shock. 9 (1982) 259−267.
[25] S.N Orlov, N.I. Pokudin, L.S. Al'Rabi, V.I. Brusovanik, A.A. Kubatiev, Biochemistry (Moscow) 58 (1993) 866−873.
[26] F.I. Ataullakhanov, V.M. Vitvitsky, A.B. Kiyatkin, A.V. Pichugin, Biophysics (Moscow) 38 (1993) 809−821.
[27] F.I. Ataullakhanov, M.V. Martinov, V.M. Vitvitsky, A.B. Kiyatkin, A.V. Pichugin, in: H.V. Westerhoff, J.L. Snoep, J.E. Wijker, B.N. Kholodenko (Eds.), Biothermokinetics of the Living Cell, BioThermoKinetics Press, Amsterdam, 1996c, pp. 80−84.
[28] F.I. Ataullakhanov, S.V. Komarova, V.M. Vitvitsky, J. Theor. Biol. 179 (1996a) 75−86.
[29] F.I. Ataullakhanov, S.V. Komarova, M.V. Martinov, V.M. Vitvitsky, J. Theor. Biol. 183 (1996b) 307−316.
[30] G. Gardos, Acta Physiol. Acad. Sci. Hung. 15 (1959) 121−125.

[31] J.A. Halperin, C. Brugnara, A. Nicholson-Weller, J. Clin. Invest. 83 (1989) 1466−1471.

[32] J.A. Halperin, A. Taratushka, M. Rynkiewicz, A. Nicholson-Weller, Blood 81 (1993) 200−205.

[33] I.S. Luganova, M.N. Blinov, K.M. Abdulkadirov, Prob. Gematol. Pereliv. Krovi 21 (11) (1976) 26−29.

[34] E. Jordanova, G. Arnaudov, Vutr. Boles. 20 (2) (1981) 119−123.

[35] T.I. Shinkareva, V.V. Punga, Probl. Tuberk (in Russian) 49 ( 11) (1971) 19−23.

[36] V.A. Martinov, I.M. Rosly, O.V. Kolobaeva, V.I. Kolobaev, N.I. Agapova, A.K. Rachkov, Ter. Arkh (in Russian) 68 (11) (1996a) 40−44.

[37] V.A. Martinov, I.M. Rosly, O.V. Kolobaeva, Vopr. Med. Khim. (in Russian) 42 (1) (1996b) 82−90.

[38] M.A. Lichtman, D.R. Miller, J. Lab. Clin. Med. 76 (1970) 267−279.

[39] C.H. Wallas, Br. J. Haematol. 27 (1974) 145−152.

[40] G.L. Dale, Adv. Biosci. 81 (1991) 41−49.

[41] F.I. Ataullakhanov, V.M. Vitvitsky, S.V. Komarova, E.V. Mosharov, Biochemistry (Moscow) 61 (1996d) 197−203.

[42] S.V. Komarova, V.M. Vitvitsky, E.V. Mosharov, M.V. Martinov, F.I. Ataullakhanov, in: H.V. Westerhoff, J.L. Snoep, J.E. Wijker, B.N. Kholodenko (Eds.), Biothermokinetics of the Living Cell, BioThermoKinetics Press, Amsterdam, 1996, pp. 101−103.

[43] T. Leinders, R.G.D.M. Van Kleef, H.P.M. Vijverberg, Biochim. Biophys. Acta 1112 (1992) 67−74.

[44] T.J.B. Simons, J. Physiol. 256 (1976) 227−244.

[45] V.L. Lew, H.G. Ferreira, Nature 263 (1976) 336−338.

[46] M. Brumen, R. Heinrich, Biosystems 17 (2) (1984) 155−169.

[47] A. Werner, R. Heinrich, Biomed. Biochim. Acta 44 (1985) 185−212.

[48] L.J. Beiling, G.G. Knight, A.D. Munro-Faure, J. Anderson, J. Clin. Invest. 45 (1966) 1817−1825.

[49] J. Funder, J.O. Wieth, Scand. J. Lab. Invest. 18 (1966) 167−180.

[50] J.A. Halperin, C. Brugnara, A.S. Kopin, J. Ingwall, D.C. Tosteson, J. Clin. Invest. 80 (1987) 128−137.

[51] A.P. Quintanilla, M.I. Weffer, H. Koh, M. Rahman, A. Molteni, F. Del Greco, Clin. Sci. 75 (1988) 167−170.

[52] G.B. Segel, S.A. Feig, B.E. Glader, A. Muller, P. Dutcher, D.G. Nathan, Blood 46 (1975) 271−278.

[53] M. Brumen, R. Heinrich, Biosystems 17 (1984) 155−169.

[54] I. Rapoport, S. Rapoport, D. Maretzki, R. Elsner, Acta Biol. Med. Germ. 38 (1979) 1419−1429.

[55] F.I. Ataullakhanov, V.M. Vitvitsky, A.M. Zhabotinsky et al., Eur. J. Biochem. 115 (1981) 359−365.

[56] T.J.B. Simons, J. Physiol. 318 (1981) 38−39.

[57] J.S. Wiley, C.C. Shaller, in: Hercules, J (Ed.), Proceedings of the First National Symposium on Sickle cell Disease, DHEW publication NIH 75−723, Bethesa, Maryland, 1977.

[58] H.G. Ferreira, V.L. Lew, J. Physiol. 252 (1975) 86−87P.

[59] B.G. Kennedy, G. Lunn, J.F. Hoffman, J. Gen. Physiol. 87 (1986) 47−72.

[60] F.I. Ataullakhanov, V.N. Buravtsev, V.M. Vitvitsky et al., Biochemistry (Moscow) 45 (1980) 817−820.

[61] P.A.G. Fortes, in: J.S. Ellory, V.L. Lew (Eds.), Membrane Transport in Red Cells, Academic Press, London, 1977, pp. 175−179.

[62] R.I. Sha'afi, in: J.S. Ellory, V.L. Lew (Eds.), Membrane Transport in Red Cells, Academic Press, London, 1977, pp. 221−256.

[63] L.I. Erlich, F.I. Ataullakhanov, V.M. Vitvitsky, A.M. Zhabotinsky, A.V. Pichugin, B.N. Kholodenko, Izv Acad Nauk Az. SSR. Ser. Biol. Nauk. 5 (1985) 754−766.

[64] H.W. Mohrenweiser, S. Fielek, K.H. Wursinger, Am. J. Hematol. 11 (1981) 125−136.

[65] A. Joshi, B.O. Palsson, J. Theor. Biol. 142 (1990a) 41−68.

[66] F.L. Meyskens, H.E. Williams, Biochem. Biophys. Acta 240 (1971) 170−179.

[67] B.M. Dean, D. Perrett, Biochim. Biophys. Acta 437 (1976) 1−15.

[68] D.E. Paglia, W.N. Valentine, M. Nakatani, R.A. Brockway, Blood 67 (1986) 988−992.

[69] G. Van den Berghe, F. Bontemps, Biomed. Biochim. Acta 49 (1990) 117−122.

[70] C. Lian, D.R. Harkness, Biochim. Biophys. Acta 341 (1974) 27−40.

[71] N. Ogasawara, H. Goto, Y. Yamada, I. Hasegawa, Adv. Exp. Med. Biol. 195A (1986) 123−127.

[72] A. Askari, S.N. Rao, Biochim. Biophys. Acta 151 (1968) 198−203.

[73] R. Sasaki, K. Ikura, H. Ciba, Agr. Biol. Chem. 40 (1976) 1797−1803.

[74] C. Solano, C.J. Coffee, Biochem. Biophys. Res. Com. 85 (1978) 564−571.

[75] R. Itoch, Biochim. Biophys. Acta 659 (1981) 31−37.

[76] G.H. Mozer, J. Schrader, A. Deussen, Am. J. Physiol. 256 (1989) C799−C806.

[77] I.I. Goryanin, in: H.V. Westerhoff, J.L. Snoep, J.E. Wijker, B.N. Kholodenko (Eds.), Biothermokinetics of the Living Cell, BioThermoKinetics Press, Amsterdam, 1996, pp. 252−253.

[78] C.W. Gear, Numerical initial value problems in ordinary differential equations, Prentice-Hall, Englewood Cliffs, N.J, 1971.